

HOLOGRAPHIC SENSORS

https://doi.org/10.1070/QEL16337

Holographic mode wavefront sensor with an enlarged number of measured modes

V.V. Orlov

Abstract. **A holographic mode wavefront sensor is proposed, which makes it possible to measure up to several tens of wavefront modes. The increase in the number of measured modes is implemented using the conversion of a light wave entering the sensor into a wide diffuse light beam, which allows one to record a large number of holograms, each intended for measuring one of the modes.**

Keywords: *holographic wavefront sensor, adaptive optics, superimposed Fourier holograms, correlation signal processing.*

1. Introduction

The purpose of wavefront sensors is to measure the wavefront shape of light waves; these devices are used in adaptive optics, ophthalmology and some other fields. Currently, a popular tool is the Shack–Hartmann sensor [1], which measures parameters related to individual wavefront regions; for this reason, this sensor belongs to devices of zonal type. The signal processing using a Shack–Hartmann sensor takes too much time to be used in adaptive optics for measuring the wavefront distortions caused by atmospheric turbulence, whose rate of variation may lie in the kilohertz range. This drawback is inherent in all zonal sensors, e.g., curvature sensors [2].

Sensors aimed at measuring the amplitudes of wavefront modes, where each mode describes the entire wavefront, are also being developed [3–6]. These sensors can provide a higher wavefront measurement rate, which is sufficient for measuring distortions caused by atmospheric turbulence. However, when designing a mode sensor, one must solve two problems. One of them is the existence of cross interferences, which arise when the wavefront shape is described by more than one mode. The second problem is the insufficiently large number of modes measured by sensor. In this paper, we describe a new holographic mode wavefront sensor, which makes it possible to measure up to several tens of wavefront modes, i.e., a much larger number of modes as compared with the previously proposed mode sensors.

2. Sensor scheme and principle of operation

The sensor contains a hologram matrix, where each hologram consists of two superimposed Fourier holograms and provides the measurement of one of the wavefront modes. The hologram matrix is recorded using a scatterer and a lens, which carries out a Fourier transform. A schematic diagram of the hologram matrix recording is presented in Fig. 1. A scatterer S is installed in the front focal plane of a lens L1, and a recording medium Md (where holograms are recorded) is located in the rear focal plane. A mobile diaphragm D1 is mounted in front of the recording medium to select a region in it for recording one of the matrix holograms. A plane wave is normally incident on the scatterer S; the phase of this wave is modulated by one of the wavefront modes, e.g., a mode set by Zernike polynomials. The diffuse light beam formed in the rear focal plane of the lens L1 is used as a reference wave for recording a hologram in the region of the recording medium Md selected by the diaphragm D1. The object wave of the hologram is a plane wave incident on the medium Md at an angle θ_1. The second hologram is recorded in the same region of the medium Md when a wave modulated by the same mode but with a phase of opposite sign is incident on the scatterer S. Here, the object wave is the second plane wave, incident on the medium Md at an angle θ_2. Then the diaphragm D1 is displaced to select another region of the recording medium, and the procedure of recording two superimposed holograms with a phase modulation of the reference wave set by another Zernike polynomial is repeated. Other holograms, recorded similarly within the diffuse beam, form the hologram matrix Mx (Fig. 2), each hologram of which consists of two superimposed holograms.

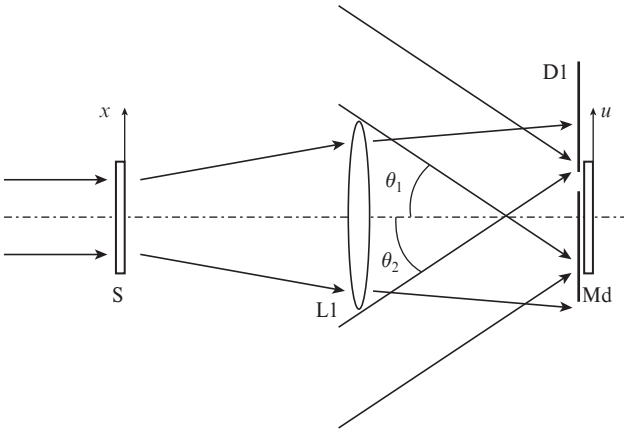

Figure 1. Schematic of the recording of a hologram matrix: (S) scatterer installed in the front focal plane of the lens L1; (D1) mobile diaphragm; (Md) medium for recording a hologram matrix, located in the rear focal plane of the lens.

V.V. Orlov ITMO University, Kronverkskiy prosp. 49, 197101 St. Petersburg, Russia; e-mail: orlov4v8v@yandex.ru

Received 10 March 2017; revision received 6 June 2017
Kvantovaya Elektronika **47** (8) 773–776 (2017)
Translated by Yu.P. Sin'kov

The scheme of the sensor is shown in Fig. 2. Along with the scatterer S, lens L1 and hologram matrix Mx, it contains two microlens rasters L. The object waves of the holograms, reconstructed when a measured wave (incident normally on the scatterer S) arrives at the sensor, enter lenses L. Diaphragms D2, which transmit the waves localised in the vicinity of the optical axes of the lenses, are installed in their rear focal planes. Photodetectors P are mounted behind the diaphragms to measure the wave intensity.

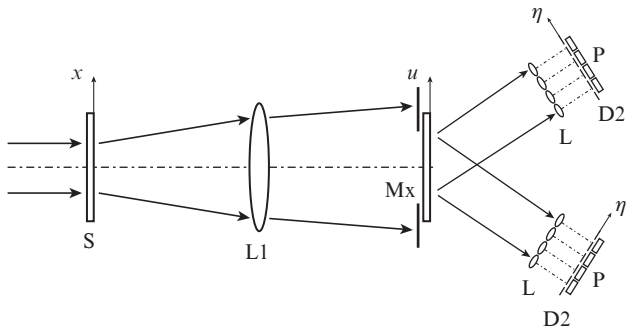

Figure 2. Schematics of the wavefront sensor:
(S) scatterer; (L1) lens; (Mx) hologram matrix; (L) microlens raster; (D2) diaphragms mounted in the microlens focal planes; (P) photodetectors.

Below we will consider the recording and reconstruction of one of the holograms of the matrix Mx. Let a plane wave be incident normally on the scatterer S with an amplitude transmittance $p(x)$. The phase of this wave is modulated by a Zernike polynomial $Z_l(x)$ with a modulation amplitude β_l. The complex amplitude of the wave transmitted through the scatterer has the form

$$R_{l1}(x) = ap(x)\exp[\mathrm{i}2\pi\beta_l Z_l(x)], \tag{1}$$

where a is the incident wave amplitude. A Fourier transform of the wave, $R_{l1}(x)$, arises in the rear focal plane of the lens L1 (in the hologram recording plane):

$$F_1[R_{l1}(x)] = R_{l1\mathrm{f}}(u) = \int_{-\infty}^{+\infty} R_{l1}(x)\exp\left(-\mathrm{i}\frac{2\pi}{\lambda f_1}ux\right)\mathrm{d}x, \tag{2}$$

where λ is the radiation wavelength and f_1 is the focal length of the lens L1. The reference wave $R_{l1\mathrm{f}}(u)$ interferes with a plane object wave $b\exp(\mathrm{i}k_1u)$ (k_1 is the wave number) incident on the recording medium at an angle θ_1 (Fig. 1). As a result, an interference pattern arises in the hologram recording plane, whose intensity can be written as

$$J_{l1}(u) = \left| R_{l1\mathrm{f}}(u) + b\exp(\mathrm{i}k_1u)\right|^2\mathrm{rect}\left(\frac{u-u_0}{d}\right), \tag{3}$$

where u_0 is the coordinate of the hologram centre and d is the hologram width, equal to the width of the diaphragm D1. Another hologram is recorded in the same region of the recording medium. It is formed by a plane object wave $b\exp(\mathrm{i}k_2u)$ incident at an angle θ_2 (Fig. 1) and a reference wave caused by the incidence of a wave $R_{l2}(x) = ap(x)\exp[-\mathrm{i}2\pi\beta_l Z_l(x)]$ on the scatterer S; according to [3], this wave differs from wave (1) by opposite phase modulation sign. As a result, two superimposed holograms are recorded, whose amplitude transmittance is proportional to the total intensity:

$$t(u) \propto J_{l1}(u) + J_{l2}(u), \tag{4}$$

where $J_{l2}(u)$ is the intensity distribution corresponding to the second hologram recording. In total, N such holograms are recorded in different regions of the recording medium with N different Zernike polynomials; these holograms form the hologram matrix Mx (see Fig. 2).

Let us assume that a measured wave $\psi(x)$, which contains both the $Z_l(x)$ mode with amplitude α_l and other Zernike modes with amplitudes γ_n, enters the sensor; this wave can be written as

$$\psi(x) \propto \exp\left\{\mathrm{i}2\pi\left[\alpha_l Z_l(x) + \sum_{n=1,\,n\neq l}^{N}\gamma_n Z_n(x)\right]\right\}. \tag{5}$$

Having passed through the scatterer S, the wave $\psi(x)$ in the rear focal plane of the lens L1 takes the form

$$\psi_\mathrm{f}(u) = F_1[p(x)\psi(x)]. \tag{6}$$

When falling on the superimposed holograms, this wave reconstructs the object waves of the holograms, which is described by the product $t(u)\psi_\mathrm{f}(u)$. The reconstructed object wave of the first superimposed hologram has the form

$$O_{l1\mathrm{f}}(u) \propto \exp(\mathrm{i}k_1u)R^*_{l1\mathrm{f}}(u)\psi_\mathrm{f}(u)\mathrm{rect}\left(\frac{u-u_0}{d}\right). \tag{7}$$

Let us simplify expression (7) by excluding the exponential taking into account the object wave propagation at an angle θ_1 with respect to the sensor optical axis. The propagating wave $O_{l1\mathrm{f}}(u)$ falls on the corresponding lens of the microlens raster L. A Fourier transform of this wave,

$$O_{l1\mathrm{L}}(\eta) \propto F_2\left[R^*_{l1\mathrm{f}}(u)\psi_\mathrm{f}(u)\,\mathrm{rect}\left(\frac{u-u_0}{d}\right)\right], \tag{8}$$

which depends on the focal length of the raster lenses, arises in the lens focal plane. Let us denote the ratio of the focal length of the lens L1 to the focal length of the raster lenses as q. Having performed necessary mathematical transformations, we arrive at

$$\begin{aligned} O_{l1\mathrm{L}}(\eta) &\propto F_2[R^*_{l1\mathrm{f}}(u)\psi_\mathrm{f}(u)] \\ &= \int_{-\infty}^{\infty} p^*(q\xi)\exp[-\mathrm{i}2\pi\beta_l Z_l(q\xi)]p[q(\xi-\eta)] \\ &\times\exp\left(\mathrm{i}2\pi\left\{\alpha_l Z_l[q(\xi-\eta)] + \sum_{n=1,\,n\neq l}^{N}\gamma_n Z_n[q(\xi-\eta)]\right\}\right)\mathrm{d}\xi. \end{aligned} \tag{9}$$

Expression (9) is the cross-correlation function of two functions entering (9), one with an argument $q\xi$, and the other with an argument $q(\xi-\eta)$. Note that the scheme of the sensor (Fig. 2) is similar to that of the Van der Lugt correlator [7], while its principle of operation is similar to the methods of holographic subtraction [8] and detection [9,10] of common image fragments. In order not to make expression (9) too cumbersome, we excluded the function $\mathrm{rect}[(u-u_0)d^{-1}]$ (which taking into account the hologram width d) from it. The presence of this function leads to a convolution of the

right-hand side of equality (9) with the Fourier transform of this function.

When a scatterer is used, the correlation peak of the cross-correlation function (9) is narrower than in the absence of a scatterer, when $p(x) = 1$. The use of a scatterer leads to the occurrence of a noise characteristic of holograms with an extended reference source, which are also referred to as holograms with a coded reference beam. For these holograms, the noise intensity is equal to the signal intensity (here, the signal is the correlation peak and the noise is a wide plateau of the reference-source autocorrelation function) [7, 11]. Since the number of holograms recorded with an extended reference source is $2N$, the ratio of the signal intensity from any of the superimposed holograms to the intensity of the noise (formed by all holograms) in the plane of the hologram matrix Mx does not exceed $1/2N$. It is important that the width of the spectrum of noise spatial frequencies is twice as large as the width of the spatial-frequency spectrum for a diffuse reference wave [7]. Therefore, the noise dissipates, and the overwhelming part of it is blocked by diaphragms D2 (see Fig. 2).

The amplitude of the correlation peak in its maximum (on the optical axis) at $\eta = 0$ can be written as

$$O_{l1\mathrm{L}}(0) \propto \int_{-\infty}^{+\infty} |\, p(q\xi)\,|^2 \times \exp\left\{ \mathrm{i}2\pi \left[(\alpha_l - \beta_l) Z_l(q\xi) + \sum_{n=1,\, n\neq l}^{N} \gamma_n Z_n(q\xi) \right] \right\} \mathrm{d}\xi . \quad (10)$$

Having considered in a similar way the reconstruction of the object wave of the second superimposed hologram, we find that its amplitude in the focal plane on the optical axis of the raster lens is

$$O_{l2\mathrm{L}}(0) \propto \int_{-\infty}^{+\infty} |\, p(q\xi)\,|^2 \times \exp\left\{ \mathrm{i}2\pi \left[(\alpha_l + \beta_l) Z_l(q\xi) + \sum_{n=1,\, n\neq l}^{N} \gamma_n Z_n(q\xi) \right] \right\} \mathrm{d}\xi . \quad (11)$$

Having compared expressions (10) and (11) with the expressions for the signals from other mode wavefront sensors that use the measured-wave modulation proposed in [3] (for example, with the expressions reported in [5, 12]), one can see that the signals depend identically on both the measured mode and the intermodal cross interferences [in (10) and (11), the latter are the modes outside the summation sign]. Different methods for processing signals (10) and (11) were considered in [13].

The number of holograms the hologram matrix may contain (i.e., the number of measured modes) depends on the area of the part of the diffuse beam in the focal plane of the lens L1 that contains all spatial frequencies of modes. The diffuse-beam diameter in the lens focal plane is $D_\mathrm{d} + D_\mathrm{m}$, where D_d is the diameter of the scatterer Fourier transform and D_m is the diameter of the localisation domain of the mode Fourier transform. The diameter of the beam part containing all spatial mode frequencies is $D = D_\mathrm{d} - D_\mathrm{m}$. Within the area confined by the diffuse beam diameter D, one can record no more than N holograms of diameter d, which form the hologram matrix; the number N is given by

$$N = \left(\frac{D}{d}\right)^2 . \quad (12)$$

It is expedient to use a scatterer for which the Fourier transform intensity is constant within the localisation domain as the scatterer S; in this case, the diffuse beam has a constant intensity within the area confined by the diameter D.

3. Experimental

The diffuse-beam diameter D can be determined experimentally using a setup schematically shown in Fig. 3. A mobile diaphragm D3, whose diameter is equal to the hologram diameter d, is installed in the rear focal plane of a lens L1. A lens L2 forms an image A' of a test object A (for example, a line test pattern located closely to the scatterer S) in its rear focal plane. Displacing the diaphragm D3 across the optical axis, one can find the diffuse beam diameter D within which the test-object image retains its quality.

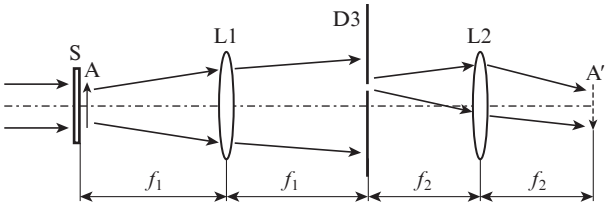

Figure 3. Schematics of the setup for determining the diffuse-beam region within which a hologram matrix is recorded:
(S) scatterer; (A) test object; (L1) lens; (D3) mobile diaphragm, installed in the rear focal plane of lens L1; (L2) lens forming an image A′ of a test object A in its rear focal plane.

This method was applied to find the diffuse-beam diameter D using a frosted glass as the scatterer S. A light beam (15 mm in diameter) with a wavelength of 632 nm was incident on the frosted glass. The diameter of the diaphragm D3 was 1 mm. An objective with a focal length of 58 mm played the role of the lens L1. Under these conditions, we observed an image of a line test pattern with a spatial frequency of 3.2 lines mm^{-1}, installed closely to the frosted glass. The test-pattern image had a speckle structure and a contrast of 0.86. The diffuse-beam diameter D, measured when displacing the diaphragm D3, was found to be 8 mm. For this D value and a hologram matrix with a hexagonal structure (Fig. 4), one can record 44 holograms with a diameter of 1 mm and, therefore, measure 44 wavefront modes. According to (12), the maximum number of holograms that can be recorded under experimental conditions is $N = 64$.

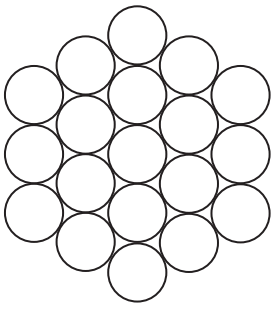

Figure 4. Hologram matrix with a hexagonal structure, containing 19 holograms.

4. Conclusions

A holographic mode wavefront sensor was proposed, which makes it possible to increase significantly (up to several tens of modes) the number of measured modes. The increase in the number N of measured wavefront modes is obtained by converting a measured light wave into a diffuse light beam; it is accompanied by a decrease in the intensity of object waves reconstructed by the holograms proportionally to $1/N$. This dependence provides a higher intensity of sensor signals in comparison with the alternative version: recording all superimposed holograms in the same region of the recording medium; in this case, the diffraction efficiency of the holograms decreases proportionally to $1/N^2$ [7].

Acknowledgements. I am grateful to V.Yu. Venediktov for the valuable discussion of the problem of designing a holographic wavefront sensor.

References

1. Platt B.C., Shack R. *J. Refractive Surg.*, **17**, S573 (2001).
2. Roddier F. *Appl. Opt.*, **27**, 1223 (1988).
3. Neil M.A.A., Booth M.J., Wilson T. *J. Opt. Soc. Am. A.*, **17**, 1098 (2000).
4. Andersen G.P., Dussan L., Ghebremichael F., Chen K. *Opt. Eng.*, **48**, 085801 (2009).
5. Dong S., Haist T., Osten W., Ruppe T., Sawodny O. *Appl. Opt.*, **51**, 1318 (2012).
6. Kovalev M.S., Krasin G.K., Malinina P.I., Odinokov S.B., Sagatelyan H.R. *J. Phys. Conf. Ser.*, **737**, 012064 (2016).
7. Colier R., Burckhardt C., Lin L. *Optical Holography* (New York: Academic, 1971; Moscow: Mir, 1973).
8. Vasilenko G.I., Tsibul'kin L.M. *Gologaficheskie raspoznayushchie ustroistva* (Holographic Recognising Devices) (Moscow: Radio i svyaz', 1985).
9. Pavlov A.V. *Quantum Electron.*, **46**, 759 (2016) [*Kvantovaya Elektron.*, **46**, 759 (2016)].
10. Pavlov A.V. *Quantum Electron.*, **47**, 335 (2017) [*Kvantovaya Elektron.*, **47**, 335 (2017)].
11. Yakimovich A.P. *Sov J. Quantum Electron.*, **5**, 348 (1975) [*Kvantovaya Elektron.*, **2**, 615 (1975)].
12. Anzuola E., Zepp A., Palomo M., Gladysz S., Stein K. *Proc. Imaging and Applied Optics 2016, OSA Tech. Digest* (Heidelberg, Germany, 2016) AOM4C.2.
13. Booth M.J. *Proc. SPIE*, **5162**, 79 (2003).